36th International Workshop on Water Waves and Floating Bodies (IWWWFB), Seoul National University, Seoul, South Korea, 25-28 April, 2021

Optimizing Wave-Generation and -Damping In 3D-Flow Simulations When Using Implicit Relaxation-Zones

Robinson Perić[1,*], Vuko Vukčević[2], Moustafa Abdel-Maksoud[1], Hrvoje Jasak[3,4]

[1]Hamburg University of Technology, Institute for Fluid Dynamics and Ship Theory, Am Schwarzenberg-Campus 1, 21073 Hamburg, Germany
[2]SimScale GmbH, Riddlerstrasse 31b, Munich, Germany
[3]University of Zagreb, Faculty of Mechanical Engineering and Naval Architecture, Ivana Lučića 5, Zagreb, Croatia
[4]Wikki Ltd, 459 Southbank House, SE1 7SJ, London, United Kingdom

[*]Corresponding author, robinson.peric@tuhh.de

1 INTRODUCTION

In finite-volume-based flow simulations with free-surface waves, accurate wave-generation and wave-damping at the domain boundaries is important. Wave reflections at the boundaries of the computational domain can cause substantial errors in the results and must therefore be minimized (cf. Perić and Abdel-Maksoud, 2016). This can be achieved by implementing *relaxation zones*, which gradually fade-out the simulated flow solution and blend-in a prescribed far-field wave solution near the domain boundaries.

The main challenge with relaxation zones is that they only provide satisfactory wave-generation and -damping *if their case-dependent parameters are optimized*. In contrast to similar approaches (such as 'forcing zones', cf. Perić, 2019), no analytical approach has been presented yet to obtain the optimum values for the case-dependent parameters of relaxation zones.

Relaxation zones can be subdivided into implicit and explicit relaxation zones, which are fundamentally different.

Implicit relaxation zones (implemented e.g. in Naval Hydro Pack, cf. Vukčević et al., 2016a, 2016b; Perić, 2019) introduce source terms in the governing equations to blend, say a general transport equation $\mathcal{T}$ for transport quantity ϕ, over to a reference solution ϕ_{ref} via

$$(1 - b(\mathbf{x}))\,\mathcal{T} + \frac{b(\mathbf{x})}{\tau}\mathcal{R} = 0 \quad , \tag{1}$$

where $b(\mathbf{x})$ is a blending function such as Eq. (5), $\mathcal{T}$ corresponds e.g. to the conservation equations for fluid momentum or volume fraction, and $\mathcal{R}$ corresponds to $\int_V (\phi_- \phi_{\text{ref}})\ \mathrm{d}V$ (cf. Sect. 2).

Explicit relaxation zones (implemented e.g. in waves2Foam, cf. Jacobsen et al., 2012) modify the fields for volume fraction α and velocity $\mathbf{u}$ by replacing computed values ϕ_{computed} by

$$\phi = (1 - b(\mathbf{x}))\phi_{\text{target}} + b(\mathbf{x})\phi_{\text{computed}} \quad , \tag{2}$$

where $b(\mathbf{x})$ is a weighting function and ϕ_{target} is the target solution. This modification is performed in each time-step, e.g. prior to the solution of the pressure-velocity coupling (cf. Jacobsen et al., 2012). In contrast to implicit relaxation zones, it is not directly apparent to which source terms in the governing equations the 'explicit' manipulation of the flow field corresponds. Therefore, in the following the focus will be on implicit relaxation zones.

The aim of this work is to present an analytical approach to optimize the case-dependent parameters of implicit relaxation zones, so that these can be optimized before performing the flow simulation.

Section 3 presents the analytical approach. Section 5 compares the analytical predictions against results from 2D- and 3D-flow simulations based on the setup from Sect. 4 and discusses the findings.

2 GOVERNING EQUATIONS WITH IMPLICIT RELAXATION ZONES

The conservation equations for momentum and volume fraction take the form

$$(1-b(\mathbf{x}))\left[\frac{\mathrm{d}}{\mathrm{d}t}\int_V \rho u_i \,\mathrm{d}V + \int_S \rho u_i(\mathbf{u}-\mathbf{u}_g)\cdot\mathbf{n}\,\mathrm{d}S - \int_S(\tau_{ij}\mathbf{i}_j - p\mathbf{i}_i)\cdot\mathbf{n}\,\mathrm{d}S - \int_V \rho\mathbf{g}\cdot\mathbf{i}_i\,\mathrm{d}V\right] + \frac{b(\mathbf{x})}{\tau}\left[\int_V \rho\left(\mathbf{u}-\mathbf{u}_{\mathrm{ref}}\right)\,\mathrm{d}V\right] = 0 \quad , \tag{3}$$

$$(1-b(\mathbf{x}))\left[\frac{\mathrm{d}}{\mathrm{d}t}\int_V \alpha\,\mathrm{d}V + \int_S \alpha(\mathbf{u}-\mathbf{u}_{\mathrm{g}})\cdot\mathbf{n}\,\mathrm{d}S\right] + \frac{b(\mathbf{x})}{\tau}\left[\int_V (\alpha-\alpha_{\mathrm{ref}})\,\mathrm{d}V\right] = 0 \tag{4}$$

with volume V of control volume (CV) bounded by the closed surface S, fluid velocity $\mathbf{u} = (u_1, u_2, u_3)^{\mathrm{T}} = (u, v, w)^{\mathrm{T}}$, grid velocity $\mathbf{u}_g$, unit vector $\mathbf{n}$ normal to S and pointing outwards, time t, pressure p, fluid density ρ, components τ_{ij} of the viscous stress tensor, unit vector $\mathbf{i}_j$ in direction x_j, volume fraction α of water, reference velocities $\mathbf{u}_{\mathrm{ref}}$ and reference volume fraction α_{ref}.

Implicit relaxation zones have three case-dependent parameters: relaxation parameter τ, blending function $b(\mathbf{x})$, and relaxation zone thickness x_{d}. The relaxation parameter τ has unit [s] and regulates the magnitude of the source term in such a way that a large value of τ implicates a small source term and vice versa[1]. The blending function is bounded between 0 and 1. In this work, power blending functions will be used

$$b(\mathbf{x}) = \left(\frac{x_{\mathrm{d}} - \tilde{x}}{x_{\mathrm{d}}}\right)^n \quad , \tag{5}$$

where $\tilde{x}$ is the shortest distance to the closest domain boundary to which a relaxation zone of thickness x_{d} is attached, and n regulates the shape of the blending function.

3 ANALYTICAL APPROACH FOR OPTIMIZING THE CASE-DEPENDENT PARAMETERS IN IMPLICIT RELAXATION ZONES

To estimate the optimum values for the case-dependent parameters in implicit relaxation zones, multiply Eqs. (3) and (4) by the factor $1/\left(1-b(\mathbf{x})\right)$. Then, the implicit relaxation zone can be interpreted as a forcing zone (cf. Perić, 2019) with forcing strength γ set to

$$\gamma = \left(\frac{\bar{E}_{\mathrm{kin},x} + \bar{E}_{\mathrm{kin},y} + \bar{E}_{\mathrm{kin},z} + \bar{E}_{\mathrm{pot}}}{\bar{E}_{\mathrm{kin},x}}\right)\frac{1}{\tau(1-b(\mathbf{x}))} \quad , \tag{6}$$

with kinetic $\bar{E}_{\mathrm{kin},x_i}$ and potential $\bar{E}_{\mathrm{pot}}$ wave energy components, relaxation parameter τ and blending function $b(\mathbf{x})$; the analytical solution can then be taken from Perić and Abdel-Maksoud (2018).

This derivation neglects some flow phenomena of minor importance, such as that reflected wave components due to different source terms can have different phases and may partially cancel destructively. Thus, actual reflection coefficients can be lower than predicted via Eq. (6). Apart from this, the following can be expected from Perić (2019): The optimum value of relaxation parameter τ will be closely predicted. The predictions for reflection coefficient C_{R} can be taken as estimates for the upper-limit of the actual reflection coefficients in the simulations. The relaxation zones behave discretization-independent. For irregular waves, the overall reflection coefficient C_{R} can be estimated based on the reflection coefficients of each wave component. The approach applies for nonlinear waves as well, because, for optimized parameters, partial wave-reflection occurs throughout the relaxation zone with small amplitudes (i.e.

[1]Note that in some publications τ has been considered a numerical-stability parameter and has therefore occasionally been omitted from Eq. (1). However, the present work demonstrates the physical meaning of τ and also that its optimum value does not necessarily coincide with the value which gives the most favorable matrix conditioning.

nearly linear waves), which can interfere destructively. This ability to 'linearize' nonlinear waves makes these comparatively simple approaches applicable to highly nonlinear, complex flows, and this is their main advantage compared to boundary-based approaches, in which a complex nonlinear solution must be prescribed at the domain boundary. For oblique wave incidence, the analytical approach above can be extended to provide reflection coefficient C_R as a function of wave incidence angle. Results from 3D-flow simulations with strongly reflecting bodies in waves suggest that the analytical approach for 2D-wave propagation as outlined above typically suffices to optimize the relaxation zone's parameters. A simple computer program to optimize implicit relaxation zones has been published as free software: `https://github.com/wave-absorbing-layers/relaxation-zones-for-free-surface-waves`.

4 SIMULATION SETUP

Flow simulations of free-surface wave-propagation were performed based on Eqs. (3) to (4), using `foam-extend` version 4.1, an open-source solver fork of the solver OpenFOAM (Weller et al., 1998), combined with the commercial software Naval Hydro Pack. The solvers were conjugate gradient with Incomplete Cholesky preconditioner for pressures and bi-conjugate gradient with ILU0 preconditioner for volume fraction and velocities. The PIMPLE scheme was used with two pressure-correction steps per each of the two nonlinear iterations per time step. No under-relaxation was used. In all simulations, the Courant number $C = |\mathbf{v}|\Delta t/\Delta x$ was well below 0.4. Further information on the discretization of and solvers for the governing equations can be found in Ferziger and Perić (2002) and the flow solver manuals. The Volume of Fluid (VOF) method was used. Waves are generated by prescribing volume fraction and velocities according to stream function wave theory (64^{th} order). More details on the setup, including a discretization-dependence study, can be found in Perić (2019).

5 RESULTS AND DISCUSSION

Figure 1 shows results from 2D-flow simulations of regular, long-crested waves traveling towards an implicit relaxation zone. The reflection coefficient $C_\mathrm{R} = H_\mathrm{refl}/H$ in terms of reflected and generated wave heights, H_R and H, was calculated as in Perić (2019).

The results show that the optimum value for relaxation parameter τ can vary by three orders of magnitude, when zone thickness x_d and exponent n of the blending function $b(\mathbf{x})$ are varied. This demonstrates the importance of optimizing the relaxation zone's parameters. The optimum value for τ is well predicted analytically. Note that its optimum value will differ depending on the wave period T.

Figure 2 shows results from 3D-flow simulations with a semi-submerged, fixed pontoon positioned in long-crested far-field waves. The analytical optimum ($\tau = 2.5\,\mathrm{s}$) for this case produced a periodic solution, indicating that wave-generation and damping were effective. Too small τ-values produced wave reflections at the entrance to the relaxation zone, and the forces acting on the pontoon became aperiodic and increased in amplitude (cf. Fig. 2, left image). Too large τ-values damped not only the undesired wave reflections, but also the incident wave, so that the far-field wave was not maintained anymore, resulting in too low forces on the pontoon (cf. Fig. 2, right image). Detailed plots of the forces acting on the pontoon can be found in Perić (2019).

6 CONCLUSION AND ACKNOWLEDGEMENTS

The present results demonstrate that the proposed approach is suitable for optimizing the parameters of implicit relaxation zones in complex 3D-flow simulations, as demonstrated for the generic case of a strongly wave-reflecting pontoon subjected to long-crested far-field waves.

The authors gratefully acknowledge the financial support by grants AB 112/11-1 and AB 112/11-2 by the Deutsche Forschungsgemeinschaft (DFG) for this study.

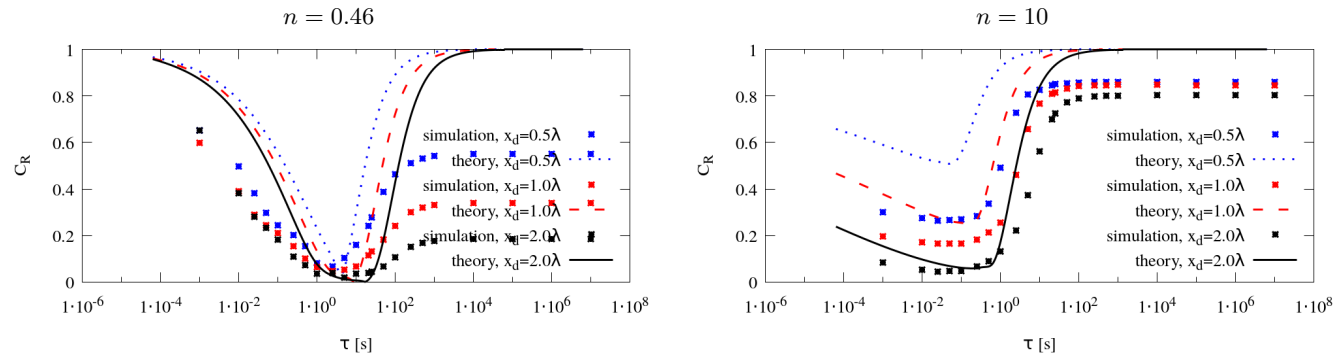

Figure 1: Analytical predictions and simulation results for reflection coefficient C_R as a function of relaxation parameter τ, for deep-water waves with period $T = 1.6\,\mathrm{s}$; for different relaxation zone thickness x_d and power blending via Eq. (5) with different values for exponent n; for all simulation results $C_\mathrm{R,sim}$ and corresponding theory predictions $C_\mathrm{R,theory}$ holds $C_\mathrm{R,sim} - C_\mathrm{R,theory} < 4.7\%$ ($n = 0.46$), and $< 2.3\%$ ($n = 10$); for the forcing strength $\tau \leq \tau_\mathrm{opt,theory}$ closest to the theoretical optimum value $\tau_\mathrm{opt,theory}$ holds $C_\mathrm{R,sim} - C_\mathrm{R,theory} < 3\%$ ($n = 0.46$), and $< -1.5\%$ ($n = 10$)

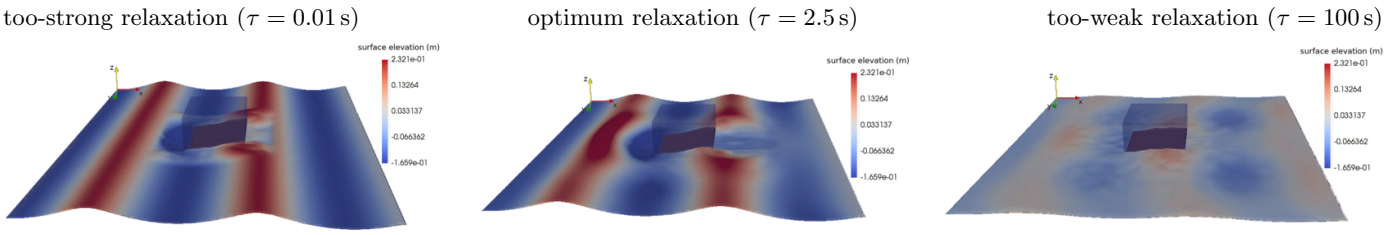

Figure 2: Simulation results for free-surface elevation at $t \approx 15\,\mathrm{s}$ with too small ($\tau = 0.01\,\mathrm{s}$), close-to-optimum ($\tau = 2.5\,\mathrm{s}$) and too large ($\tau = 100\,\mathrm{s}$) value of relaxation parameter τ; for relaxation-zone thickness $x_\mathrm{d} \approx 0.7\lambda$ and blending via Eq. (5) with exponent $n = 0.46$; if the relaxation is too strong (left), wave-reflection occurs near the entrance to the relaxation zone; if relaxation is too weak (right), the far-field wave is not sustained; for optimized relaxation-setup (middle), the waves reflected at the pontoon decay smoothly over the whole relaxation zone as intended

REFERENCES

[1] Ferziger, J. H., & Peric, M. (2002). Computational methods for fluid dynamics. Springer Science & Business Media.

[2] Jacobsen, N. G., Fuhrman, D. R., & Fredsøe, J. (2012). A wave generation toolbox for the open-source CFD library: OpenFoam®. International Journal for Numerical Methods in Fluids, 70(9), 1073-1088.

[3] Perić, R., & Abdel-Maksoud, M. (2016). Reliable damping of free-surface waves in numerical simulations. Ship Technology Research, 63(1), 1-13.

[4] Perić, R., & Abdel-Maksoud, M. (2018). Analytical prediction of reflection coefficients for wave absorbing layers in flow simulations of regular free-surface waves. Ocean Engineering, 147, 132-147.

[5] Perić, R. (2019). Minimizing undesired wave reflection at the domain boundaries in flow simulations with forcing zones. PhD-thesis at Hamburg University of Technology, Hamburg, Germany, DOI: `https://doi.org/10.15480/882.2394`.

[6] Vukčević, V., Jasak, H., & Malenica, Š. (2016a). Decomposition model for naval hydrodynamic applications, Part I: Computational method. Ocean Engineering, 121, 37-46.

[7] Vukčević, V., Jasak, H., & Malenica, Š. (2016b). Decomposition model for naval hydrodynamic applications, Part II: Verification and validation. Ocean engineering, 121, 76-88.